Atmos. Chem. Phys. Discuss., 10, 14737–14769, 2010
www.atmos-chem-phys-discuss.net/10/14737/2010/
doi:10.5194/acpd-10-14737-2010
© Author(s) 2010. CC Attribution 3.0 License.

Atmospheric Chemistry and Physics Discussions

This discussion paper is/has been under review for the journal Atmospheric Chemistry and Physics (ACP). Please refer to the corresponding final paper in ACP if available.

The importance of transport model uncertainties for the estimation of CO_2 sources and sinks using satellite measurements

S. Houweling[1,2], I. Aben[1], F.-M. Breon[3], F. Chevallier[3], N. Deutscher[4], R. Engelen[5], C. Gerbig[6], D. Griffith[4], K. Hungershoefer[3,7], R. Macatangay[4], J. Marshall[6], J. Notholt[8], W. Peters[9], and S. Serrar[5]

[1]Netherlands Institute for Space Research (SRON), Utrecht, The Netherlands
[2]Institute for Marine and Atmospheric Research Utrecht (IMAU), Utrecht University, The Netherlands
[3]Laboratoire des Sciences du Climate et de l'Environnement, Gif sur Yvette, France
[4]Centre for Atmospheric Chemistry, University of Wollongong, Australia
[5]European Centre for Medium Range Weather Forecasts (ECMWF), Reading, UK
[6]Max Planck Institute for Biogeochemistry, Jena, Germany
[7]Deutscher Wetterdienst, Offenbach, Germany

[8] Institute of Environmental Physics, University of Bremen, Germany
[9] Dept. of Meteorology and Air Quality, Wageningen University, The Netherlands

Received: 26 March 2010 – Accepted: 26 May 2010 – Published: 16 June 2010

Correspondence to: S. Houweling (s.houweling@sron.nl)

Published by Copernicus Publications on behalf of the European Geosciences Union.

ACPD
10, 14737–14769, 2010

Abstract

This study presents a synthetic model intercomparison to investigate the importance of transport model errors for estimating the sources and sinks of CO_2 using satellite measurements. The experiments were designed for testing the potential performance of the proposed CO_2 lidar A-SCOPE, but also apply to other space borne missions that monitor total column CO_2. The participating transport models IFS, LMDZ, TM3, and TM5 were run in forward and inverse mode using common CO_2 fluxes and initial concentrations. Simulated column averaged CO_2 (xCO_2) mixing ratios vary between the models by σ=0.5 ppm over the continents and σ=0.27 ppm over sea. A variable, but overall quite encouraging agreement is found in comparison with FTS measurements at Park Falls, Darwin, Spitsbergen, and Bremen. Despite the fact that the models agree on average on the sub-ppm level, these modest differences nevertheless lead to significant discrepancies in the inverted fluxes of 0.1 Pg C/yr per 10^6 km^2 over land and 0.03 Pg C/yr per 10^6 km^2 over the ocean. These transport model induced flux uncertainties exceed the target requirement that was formulated for the A-SCOPE mission of 0.02 Pg C/yr per 10^6 km^2, and could also limit the overall performance of other CO_2 missions such as GOSAT. It is concluded that to make use of the remote sensing technique for quantifying the sources and sinks of CO_2 not only requires highly accurate satellite instruments, but also puts stringent requirements on the performance of atmospheric transport models. Further development of these models should receive high priority.

1 Introduction

Eight years after Rayner and O'Brien (2001) first pointed to the potential usefulness of CO_2 monitoring from space, the Japanese space agency launched the Greenhouse gas Observing SATellite (GOSAT). Atmospheric CO_2 measurements provide important constraints on the surface exchange of carbon from regional to continental scales.

ACPD
10, 14737–14769, 2010

A satellite-mounted instrument is an attractive option for measuring CO_2 because it can extend the highly heterogeneous coverage of the surface monitoring networks to the entire globe. GOSAT (Yokota et al., 2004) is the first instrument in orbit that is designed to measure the CO_2 mixing ratio at sufficient accuracy and sensitivity down to the Earth's surface to allow world-wide estimation of regional sources and sinks of CO_2.

After Rayner and O'Brien (2001) several studies have been carried out to investigate the various options for measuring CO_2 from space and to determine what can be expected from this approach (Pak and Prather, 2001; Rayner et al., 2002; Houweling et al., 2004; Baker et al., 2006a; Chevallier et al., 2007; Miller et al., 2007; Feng et al., 2009). A common method for estimating instrument performance is to determine the reduction in surface flux uncertainty that can be gained by inverse modelling of hypothetical satellite measurements. These so called Observing System Simulation Experiments (OSSEs) are fully theoretical, although the boundary conditions specifying e.g. the surface fluxes and the satellite measurements are designed to mimic a real-world application as much as possible. A major limitation of this approach is that it is difficult to account, in a realistic manner, for correlated uncertainties and bias. In the data-rich world of satellite instruments the estimation of CO_2 fluxes is highly sensitive to the treatment of such errors (see for example Ehret and Kiemle, 2005; Kadygrov et al., 2009; Chevallier et al., 2006; Chevallier, 2007).

A potentially important contributor to correlated uncertainty and bias is the atmospheric transport model, which is used to translate information on CO_2 concentrations to CO_2 fluxes. Concerns have been raised about how well the available transport models, that have been validated mostly using surface measurements, can simulate the vertical column weighted average CO_2 mixing ratio (xCO_2) that is provided by satellites (Chahine et al., 2008; Buchwitz et al., 2007; Yang et al., 2007). Because of the complexity of transport model algorithms and the limited availability of quantitative information on the accuracy of the various processes involved, it is not feasible to assess transport model uncertainties using formal error propagation methods. A more prac-

ACPD
10, 14737–14769, 2010

tical approach is to organize a model-intercomparison using an experimental protocol which specifies common boundary conditions. This approach has been applied successfully in several studies of the TRANSCOM project (Denning et al., 1999; Engelen et al., 2002; Gurney et al., 2002; Baker et al., 2006b; Law et al., 2008; Patra et al., 2008). Regarding total column CO_2, transport model uncertainties have been investigated by Yang et al. (2007) and Macatangay et al. (2008) who compared model simulations with Fourier Transform Spectrometry (FTS) measurements of xCO_2. Yang et al. (2007) point to an underestimation of the model-simulated seasonal cycle of xCO_2, which is attributed to a combination of errors in surface fluxes and the vertical mixing. So far, however, no attempt has been made to estimate the potential significance of such differences for the estimation of sources and sinks using satellite measurements.

This study was initiated by ESA as a feasibility study for the A-SCOPE mission. The CO_2 lidar A-SCOPE was investigated as a prephase A Earth Explorer Mission (see Ingmann, 2009). The proposed instrument made use of a pulsed laser operating in the short wave infrared (SWIR). In theory, a pulsed laser with a small ground spot size (<100 m) is attractive because it provides accurate information on the optical path-length, a major source of uncertainty for passive measurement techniques, and is able to obtain clear sky measurements in broken cloud fields. This in combination with the fact that A-SCOPE is not limited by the availability of sunlight leads to a superior measurement coverage in comparison with passive instruments operating in the same wavelength range (such as GOSAT-TANSO). We have conducted model intercomparison experiments to i) quantify the uncertainty of model-simulated xCO_2, and ii) determine the impact of transport model errors on inverse modelling-derived CO_2 sources and sinks. The results of these experiments are used to assess the extent to which the quality of the current generation of transport models would limit the overall performance of A-SCOPE in quantifying regional sources and sinks of CO_2.

This study is organized as follows: Section 2 describes the experimental protocol and the transport models that took part in the intercomparison. Sections 3.1 and 3.2 present comparisons between forward model simulations and FTS measurements to

ACPD
10, 14737–14769, 2010

verify that the experimental set-up is realistic and to characterize and quantify transport model errors globally. Results of inverse model calculation are presented in Sect. 3.3, which are used to construct a global map of transport model-induced flux uncertainties. The main outcome of this study is discussed and summarized in Sects. 4 and 5.

2 Experimental set-up

2.1 General outline

CO_2 sources and sinks are estimated from atmospheric concentration measurements by combining the available information on CO_2 concentrations and fluxes using Bayes' law of conditional probability (see e.g., Tarantola, 2005). Following this approach, the CO_2 sources and sinks are estimated by optimizing the conditional (a posteriori) probability of the fluxes, which corresponds to minimizing the cost function

$$J(\boldsymbol{x}) = (\boldsymbol{y} - \mathbf{H}\boldsymbol{x})^T \mathbf{R}^{-1} (\boldsymbol{y} - \mathbf{H}\boldsymbol{x}) + (\boldsymbol{x} - \boldsymbol{x}^b)^T \mathbf{B}^{-1} (\boldsymbol{x} - \boldsymbol{x}^b) . \quad (1)$$

Vector $\boldsymbol{x}$ represents the parameters to be estimated (i.e. CO_2 fluxes and initial concentrations), on the basis of the prior information $\boldsymbol{x}^b$ and measurements $\boldsymbol{y}$, weighted by the covariance matrices **B** and **R**. Operator **H** quantifies the sensitivity of the observed concentrations towards the fluxes as derived from atmospheric transport models. In applications involving satellite data the dimensions of the cost function are computationally too large to handle by matrix algebra. Several techniques have been developed to deal with this problem, including the variational technique and ensemble Kalman filtering (Chevallier et al., 2005; Peters et al., 2007; Meirink et al., 2008a). The variational technique makes use of the adjoint of the transport model to probe gradients of the cost function by an iterative procedure converging towards the minimum (see e.g., Meirink et al., 2008a).

Covariance matrix **R** accounts for several sources of error as expressed by

$$\mathrm{R} = \mathrm{R}_d + \mathrm{R}_m + \mathrm{R}_r , \quad (2)$$

ACPD
10, 14737–14769, 2010

where $\mathbf{R}_d$ represents the measurement uncertainty, $\mathbf{R}_m$ the transport model uncertainty, and $\mathbf{R}_r$ the representativeness error caused by comparing measurements and simulations that do not represent the same volume of air. As explained earlier, $\mathbf{R}_m$ is difficult to represent in a realistic manner not only because transport model uncertainties are poorly quantified but also because, unlike $\mathbf{R}_d$ and $\mathbf{R}_r$, its off-diagonal terms are expected to contribute significantly.

We isolate the role of $\mathbf{R}_m$ by designing a purely synthetic model intercomparison experiment in which all initial and boundary conditions are prescribed by an experimental protocol adopted by each model. In the first step the models were run in forward mode and sampled according to the orbit and measurement characteristics of the A-SCOPE instrument, including its vertical weighting function (see Sect. 2.3). The differences between the models have been analyzed and results were compared with available FTS measurements. In the second step, surface fluxes were estimated by inverse modelling using A-SCOPE samples that were generated by a different model than used in the inversion. The difference between the posterior and prior fluxes is caused by transport model differences only. It was verified that the inversion set-up is consistent with the forward model simulation in the sense that no flux adjustments should be found when inverting the data generated by the same model as used in the inversion. A practical approach, which guarantees that this requirement is satisfied, is to invert for the difference between two sets of forward model-generated samples, setting the prior fluxes and initial concentrations in the inversion to zero.

2.2 Transport models and optimization tools

Table 2 lists the atmospheric transport models that participated in the model intercomparison experiment and provides some general characteristics. Since the IFS model only contributed forward model simulations, 3 inverse models were run using synthetic A-SCOPE samples generated by 3 other models. Strictly speaking, since the grid definitions of the models differ, the estimate of $\mathbf{R}_m$ derived from the intercomparison inevitably includes some contribution of $\mathbf{R}_r$. However, considering that A-SCOPE was

ACPD
10, 14737–14769, 2010

designed to have a footprint of only ∼100 m this should only make a small contribution to the overall $\mathbf{R}_r$. The statistical interpretation of the result of the experiment would obviously benefit from an ensemble of transport models that spans the range of transport model uncertainty. Unfortunately, this is not the case in our experiment since 3 out of 4 make use of meteorological fields from the ECMWF model. As expected, comparisons with in-situ CO_2 measurements indicate that the models agree better with each other than with the measurements (Breon et al., 2009). Nevertheless, substantial scatter between the models remains (see e.g., Breon et al., 2009; Law et al., 2008), so that the model ensemble should at least represent a major component of the real uncertainty.

All optimization algorithms make use of the variational technique, although the preconditioning and search methods differ between the implementations (for details see Meirink et al., 2008b for TM5, Rödenbeck et al., 2003 for TM3, and Chevallier et al., 2005 for LMDZ). A-SCOPE samples were generated for the year 2005. Forward and inverse model calculations start at 1 December 2004 to allow for 1 month spin-up time. Surface fluxes are estimated for the full period. The inverse calculations were terminated after 60 iterations. This is not considered sufficient for calculating a posteriori uncertainties, however, most relevant for this study is the solution itself of which the main characteristics converged within 60 iterations.

2.3 Common boundary conditions

The main requirement for the boundary conditions is that they lead to a reasonably realistic simulation of xCO_2, so that the outcome of the experiment can be considered representative of a real-world application. As an additional advantage of a realistic choice of boundary conditions the model performance can be evaluated against measurements. This is of particular relevance for this study since the performance of transport models with respect to total column CO_2 has not yet been well established. For this reason, we prescribed surface fluxes that were generated by CarbonTracker (Peters et al., 2007). These fluxes have been optimized using flask and in-situ measurements from many sites of the NOAA network, which guarantees that the large-scale

ACPD
10, 14737–14769, 2010

concentration variations near the surface remain in fairly close agreement with reality.

Table 3 summarizes the main assumptions and data sets that were used for the experiments. The initial concentrations at the start of the simulation were derived from a TM5 run which started 3 years earlier, using meteorological fields and CarbonTracker fluxes corresponding to those years. The inversion solves for the initial value of xCO_2 for each vertical column in the domain, using an a priori uncertainty of 3.8 ppm (1%) and an exponentially decaying spatial correlation with an e-folding length-scale of 1000 km. The prior flux uncertainties were distributed proportional to heterotrophic respiration over land and were kept constant for the ocean. For the latter, it would have been more realistic to assume increased uncertainties at higher latitudes of both hemispheres. However, since the uncertainty over the ocean is substantially smaller than over land, the inverted fluxes are not sensitive to the assumed pattern of uncertainty over sea. The prior flux uncertainty and its correlation length-scales in space and time are similar to what has been assumed in previous studies. We verified that our uncertainties integrated over TRANSCOM regions correspond fairly well with what was assumed by Baker et al. (2006b). The globally and annually integrated uncertainties amount to 3 Pg C/yr over land and 1 Pg C/yr over the ocean.

A-SCOPE samples were generated by simulating the polar dusk-dawn orbit of A-SCOPE accounting for cloud cover. Since A-SCOPE carries its own light source in the form of a laser it is capable of measuring year-around at high latitudes, and on both sides of the globe. A single A-SCOPE measurement consists of laser soundings integrated over a 50 km transect. The accuracy of each 50 km average measurement has been set to the target precision requirement for the A-SCOPE instrument of 0.5 ppm for a laser operating at λ=1.6 µm. The globally uniform vertical weighting function has been applied, which was calculated for A-SCOPE measurements at this wavelength (Breon et al., 2009). It is approximately uniform in the troposphere, in the sense that each CO_2 molecule in the column receives about equal weight, and decreases towards lower pressures in the stratosphere.

ACPD
10, 14737–14769, 2010

3 Results

3.1 Forward modelling: comparison to FTS measurements

Timeseries of xCO_2 have been extracted from the forward model simulations for the coordinates of the FTS sites listed in Table 1. The ability to compare models and measurements for the year 2005 is limited by the rather low number of measurements for all sites, with the exception of Park Falls. Therefore, for each site except Park Falls, the seasonal cycle for 2005 has been reconstructed from the full measured time series spanning several years. Data for other years have been used after correction for the global growth rate of CO_2, derived from linear interpolation of the average annual growth rates reported for Mauna Loa (http://www.esrl.noaa.gov/gmd/ccgg/trends/). In the case of Darwin, this correction also accounts for a recognized small drift in the measurements due to a gradual change in instrument lineshape that occurred between 2005 and 2009. Growth-rate corrected measurements have been binned in half monthly time intervals and averaged. For Park Falls, daily averaged measurements for the year 2005 have been used.

The results (see Fig. 1) show a variable, but overall very reasonable agreement between models and measurements. At Park Falls, Bremen, and to a lesser extent Spitsbergen, the models tend to underestimate the amplitude of the seasonal cycle (up to 1.5 ppm for Park Falls). The best agreement, considering both seasonal amplitude and phasing, is found at Spitsbergen. Note that the annual coverage of the FTS measurements at Spitsbergen is limited by low sun angles or even absence of sunlight during part of the year. At Park Falls and Bremen the modelled spring time maximum is phase-shifted by about half a month compared with the measurements. At all sites, the models are in fairly close agreement with each other. The 1 σ variation of the model-to-model differences at Park Falls for the whole year of 2005 amounts to $\sim$1 ppm.

The observed seasonal cycle at Darwin is less well captured by the models. The models show a second seasonal minimum in September, which is seen in the sur-

ACPD
10, 14737–14769, 2010

face measurements at Darwin (GLOBALVIEW-CO2, 2009) collected between 1992 and 1998. The total column measurements show a cessation of growth, but no decrease in CO_2 at this time of year. The agreement between the transport models suggests that the deviation between the observed and modelled seasonal cycle is caused by inaccuracies in the prescribed surface fluxes. The CarbonTracker-derived surface fluxes are indeed poorly constrained by surface measurements in this part of the Earth. The systematic offset between model and measurements may also be partially explained (up to 0.2%) by the uncertainty in the TCCON-wide calibration factors (0.990±0.002), of which Darwin lies at the lower end of the range (Deutscher et al., 2010). The IFS model slowly diverts from the other models during the year. This difference is seen at the other sites too but is most pronounced in the tropics. It is explained by the fact that the semi-lagrangian advection scheme used in IFS is not fully mass conservative. The IFS results that are used in the remainder of this study are based on a different IFS simulation using a mass fixer. The reason for showing the uncorrected version here is to demonstrate the importance of mass conservation for the simulation of total column CO_2.

The relatively high data density that is available for the Park Falls FTS allows us to focus on specific parts of the year to analyze the observed short-term variations. Figure 2 shows a comparison for the period August–October, after correction for the offset between model and measurements. It turns out that much of the observed variability is reproduced by the models. As suggested by Parazoo et al. (2008) these CO_2 variations are associated with the passage of frontal systems. Keppel-Aleks et al. (AGU fall conference presentation, 2008) demonstrated that these variations are well correlated with potential temperature and that the amplitude scales with the CO_2 north-south gradient. The good agreement in Fig. 2 can be understood by the fact that the models are at high enough resolution to at least partially resolve frontal weather systems and the fact that they capture the large-scale CO_2 gradients through the use of the optimized CarbonTracker fluxes.

ACPD
10, 14737–14769, 2010

3.2 Model intercomparison: results of forward modeling

In this section we extend the model comparison to the whole globe and shift our attention to the model-generated A-SCOPE samples. Figure 3 shows the large-scale seasonal concentration gradients of xCO_2 as simulated by the models. The values represent the mean of the samples of all models collected on a regular 1° by 1° grid. As can be seen, according to the models, global and seasonal xCO_2 spans a range of 10–15 ppm. After three months' time only a few grid boxes that experienced persistent cloud cover have not been sampled. This applies also to the poles, which are not measured due to the slight inclination of the A-SCOPE orbit.

Figures 4 and 5 show how each model deviates from the mean of all models for July and December 2005. For model-to-model differences we prefer to present the monthly, rather the seasonal, time scale to avoid averaging out differences between individual samples. The mean size of the model-to-model differences is about 0.5 ppm over the continents and about a factor of 2 lower over sea. This is somewhat smaller than the 1 ppm average difference between the modelled time series at Park Falls presented in Sect. 3.1, which can partially be explained by the monthly averaging to 1° by 1°. The largest differences are found over the interior of the North American and Asian continents, and the intertropical convergence zone over tropical Africa where the concentration gradients are relatively large as well. Generally, the results confirm a substantial spatial coherence of transport model differences. As we will see in Sect. 3.3 this has important consequences for the estimation of CO_2 sources and sinks.

3.3 Model intercomparison: results of inverse modeling

As described in Sect. 2.1 the model-generated samples that were presented in the previous section have been utilized for inverse model calculations. Figure 6 shows examples of how differences between samples generated by the TM3, LMDZ, and TM5 models are projected on the fluxes by the TM5 inversion. As expected, corresponding patterns show up when comparing monthly-averaged A-SCOPE samples

ACPD
10, 14737–14769, 2010

and inversion-derived fluxes. The mapping is not necessarily one to one, since the measurements are not only influenced by fluxes for the same month (as shown in Fig. 6) but also by fluxes from earlier months. In addition, the flux pattern is influenced by other factors such as atmospheric transport, and spatially non-uniform prior flux uncertainties.

Figure 7 shows some examples of how different inversions translate the same xCO_2 differences into fluxes. Generally it is not expected that these inversions will yield identical flux patterns. Besides the fact that the transport model plays a different role in forward and inverse mode, it is difficult to fully harmonize the inverse problem. For example, differences arise from the fact that the inversions solve the surface fluxes at different spatial resolutions. The local flux uncertainties in Table 3 are used at the model grid scale which formally leads to prior uncertainties that are a function of model resolution. However, because the correlation length scales are either similar or larger than the size of the model grid boxes, this is expected to have only a minor impact. Differences in the search algorithms used to find the minimum of the cost function should cause differences too, since the solutions do not fully converge within 60 iterations. Nevertheless, Fig. 7 shows many similarities between the flux fields generated by the TM3 and TM5 inversions. More critical for assessing the importance of transport model error is that the typical size of the flux adjustments is robust across the inversions. The results presented in Fig. 7 confirm that this is the case.

In total, nine sets of posterior fluxes are obtained from three inversions using synthetic measurements generated by three other models. In order to summarize and generalize the outcome of these inversions, annually integrated flux maps have been regridded to a common resolution of 10° by 10°, which corresponds to the scale for which the A-SCOPE requirements were specified. This leads to nine global CO_2 flux maps from which standard deviations have been calculated for each 10°×10° grid box. The resulting map (see Fig. 8) can be interpreted as the flux uncertainty arising from transport model uncertainties. As expected, the errors are larger over land than over sea, because the larger prior flux uncertainty over land increases the relative weight

ACPD
10, 14737–14769, 2010

of the measurements. Although the prior flux uncertainty is largest in the tropics, the transport model uncertainty shows substantial impact in the extra-tropics also. One should be careful, however, not to over-interpret this map because several features could be traced back to results from individual inversions, and therefore regional scale variations are probably not robust. More important is the size of the errors, which is typically of the order of 0.1 Pg C/yr per 10^6 km^2 over land and 0.03 Pg C/yr per 10^6 km^2 over the ocean. These numbers can be compared directly with the A-SCOPE requirement for the accuracy of the estimated CO_2 sources and sinks, which amounts to 0.02 Pg C/yr per 10^6 km^2 (corresponding to 20 g C m^{-2} yr^{-1} at this spatial scale). It means that the contribution from transport model error alone already exceeds the A-SCOPE requirement for the overall error.

4 Discussion

The main outcome of Sect. 3.3 is that if the A-SCOPE instrument would operate today according to its instrument requirements then the quality of the transport models would limit the overall performance in a way that would preclude achievement of the A-SCOPE mission objectives. Although the experiments were specifically designed to test A-SCOPE, similar results would be obtained for other sensors targeting the CO_2 absorption lines in the short-wave infrared including GOSAT. It should be realized, however, that the A-SCOPE mission requirements were more ambitious than those of GOSAT, and therefore the transport model performance should be less critical in the case of GOSAT.

This result is obtained despite the fact that the model-to-model differences for xCO_2 are comparable to the assumed A-SCOPE measurement precision. It has been verified that if the data uncertainty consisted of a random instrument error only, i.e. the impact of systematic error would not limit the overall performance as was required for A-SCOPE, then the target mission objective of 0.02 Pg C/yr per 10^6 km^2 would be reached (Ingmann, 2009). It means that model errors influence the sources and sinks

ACPD
10, 14737–14769, 2010

about 5 times more effectively than random instrument errors. The difference can only be explained by the non-random nature of transport model errors, which confirms earlier concerns about the potential impact of systematic errors in CO_2 measurements from satellites on inversion-derived sources and sinks (Houweling et al., 2005; Chevallier, 2007; Kadygrov et al., 2009)

In practical applications the influence of model error will be less than in our experiments, because our inversions only account for the instrument contribution to the data covariance matrix **R**. By including assumptions on the representativeness error and transport model error the measurements receive less weight, which also deweights the influence of model error. In this case, the inversion-derived posterior uncertainties represent the true uncertainties more realistically, at the cost however of a reduced precision of the flux estimates. Our experiments provide information that could be used for estimating $\mathbf{R}_m$ in Eq. (2), although it is not easy to account for the spatially and temporally varying transport model covariance in a realistic manner. On average the e-folding length scale in space amounts to about 4000 km, with some variation between the seasons. In time, the correlation shows a minimum for the analyzed period of one year at about 6 months amounting to r=~0.5. These numbers confirm the importance of systematic contributions to the overall transport model error.

Clearly, a more constructive approach to reduce the impact of transport model errors is to improve the models themselves. We have investigated which part of the vertical column contributes most to the error in $x\mathrm{CO}_2$ (not shown). Generally, the correlation between the error at a specific level and the error in $x\mathrm{CO}_2$ increases towards the surface, where the CO_2 concentration gradients are largest. This correlation breaks down within the planetary boundary layer (PBL), which can be explained by the fact that $x\mathrm{CO}_2$ is not very sensitive to variations in the PBL-height for a vertical weighting function that is close to uniform, whereas the PBL CO_2 concentration is usually highly sensitive to PBL height. It is still important to realistically represent the planetary boundary layer dynamics, since errors in the vertical CO_2 profile can be advected in different horizontal directions in the presence of wind shear.

ACPD
10, 14737–14769, 2010

A highly systematic contribution to model-to-model differences in xCO_2 has its origin in the stratosphere, and is caused by differences in the mean residence time of stratospheric air. Commonly the vertical weighting functions in the SWIR decrease towards higher altitudes in the stratosphere. However, this reduced sensitivity does not imply that stratospheric dynamics are unimportant for the interpretation of A-SCOPE or GOSAT measurements. The time-scale of stratosphere-troposphere exchange determines the effective volume into which the surface emissions are mixed, which influences CO_2 in the troposphere too.

It should be realized that the projected impact of transport model uncertainty does not account for transport model bias. Yang et al. (2007) point to a seasonal bias between the Park Falls FTS measurements and models that participated in the TRANSCOM continuous experiment. Unlike this study, the fluxes that were used in their models were not optimized using measurements from the surface network. CO_2 is a difficult tracer to evaluate atmospheric transport models, because its surface fluxes are uncertain. Flux optimization does not eliminate this problem, but it leads to an overall realistic simulation of the seasonal cycle near the surface. Any remaining mismatch in xCO_2 points to an error in transporting surface variations upwards. Yang et al. (2007) report that the TRANSCOM models underestimate the seasonal cycle at Park Falls by 34%. Our models, with optimized fluxes, still underestimate the observed seasonality by 30% despite the fact that they closely reproduce the annual cycle close to the surface, as measured from the LEF tall tower. As a sensitivity test, we accounted for the seasonal variation in the FTS vertical weighting function as reported by Bösch et al. (2006), which could not explain the remaining difference. Besides transport model errors, it can't be ruled out that some fraction of the 30% (=1.5 ppm) difference in seasonal amplitude is caused by remaining spectroscopic errors, some of which are known to introduce airmass dependencies. Jiang et al. (2008) point to an underestimation of transport model-simulated seasonal cycles in the free troposphere between 25° N and 35° N from a comparison with data from the CONTRAIL airline measurement program (Matsueda et al., 2002). Our models, however, do not show seasonal amplitudes at

ACPD
10, 14737–14769, 2010

10 km altitude that are significantly different from the 4.5 ppm as measured at those latitudes.

5 Conclusions

This study presents results of a model intercomparison experiment to investigate the role of transport model error in inverse modelling of CO_2 sources and sinks using satellite measurements. Synthetic measurements have been generated by all participating models using common initial concentrations and surface fluxes. Inverse modelling calculations have been carried in which each inversion used the measurements generated by the other models. Measurements were specified according to instrument characteristics and orbit parameters of the candidate ESA Earth Explorer mission A-SCOPE.

The contribution of transport model errors to the uncertainty of the estimated sources and sinks is on the order of 0.1 Pg C/yr per 10^6 km^2. This number exceeds the A-SCOPE target requirement by a factor of 5, indicating that if the instrument would operate today according to its instrument requirements then the transport model would be an important factor limiting the accuracy of the derived sources and sinks. Similar results would be obtained for other instruments such as GOSAT, although at the GOSAT measurement precision the influence of transport model uncertainties will be less dominant.

Despite the significance of transport model errors for estimating sources and sinks of CO_2 the model-to-model differences in simulated xCO_2 are only on the order of 0.5 ppm. The large sensitivity to model uncertainties is explained by the covariance of the transport model errors in space and time. Encouraging agreement is found between model-simulated xCO_2 and available FTS observations, although systematic differences are found exceeding the 0.5 ppm level. The models tend to systematically underestimate the observed amplitude of the seasonal cycle, by up to 30% (or 1.5 ppm) in the case of Park Falls. Besides transport model errors, errors in the surface fluxes and remaining spectroscopic uncertainties may contribute to these differences. If a sig-

ACPD
10, 14737–14769, 2010

nificant fraction is caused by transport model errors, our experiments suggest that this should have important implications for the estimation of CO_2 sources of sources using satellite measurements.

To make optimal use of the remote sensing technique for quantifying the sources and sinks of CO_2 not only requires highly accurate satellite instruments, but also puts stringent requirements on the performance of atmospheric transport models. Further development of these models should receive high priority. Ideally transport models should be evaluated using tracers that specifically address certain aspects of transport. In the absence of a suitable tracer for the total column, xCO_2 will probably be the choice of preference. This calls for an improvement in the accuracy of ground-based FTS measurements to a level well below 0.5 ppm, in combination with a detailed understanding of the surface CO_2 exchange in the vicinity of the measurement site.

Acknowledgements. We would like to thank Paul Ingmann (ESA) and his team and Andrzej Klonecky (Noveltis) for their efforts organizing this study, which was financed by ESA under contract no. 20839. The Park Falls FTS measurements are supported by Caltech, JPL, and NASA. The Darwin solar measurements and TCCON are funded by NASA's terrestrial carbon cycle program, grant NNX08AI86G.

References

Baker, D. F., Doney, S. D., and Schimel, D. S.: Variational data assimilation for atmospheric CO_2, Tellus, Ser. B, 58, 359–365, 2006a. 14740

Baker, D. F., Law, R. M., Gurney, K. R., Rayner, P., Peylin, P., Denning, A. S., Bousquet, P., Bruhwiler, L., Chen, Y.-H., Ciais, P., Fung, I. Y., Heimann, M., John, J., Maki, T., Maksyutov, S., Masarie, K., Prather, M., Pak, B., Taguchi, S., and Zhu, Z.: TransCom 3 inversion intercomparison: Impact of transport model errors on the interannual variability of regional CO_2 fluxes, 1988–2003, Global Biogeochem. Cy., 20, GB1002, doi:10.1029/2004GB002439, 2006b. 14741, 14745

Bösch, H., Toon, G. C., Sen, B., Washenfelder, R. A., Wennberg, P. O., Buchwitz, M., de Beek, R., Burrows, J. P., Crisp, D., Christi, M., Connor, B. J., Natraj, V., and Yung, Y. L.: Space-

ACPD

10, 14737–14769, 2010

based near-infrared CO_2 measurements: testing the orbiting carbon observatory retrieval algorithm and validation concept using SCIAMACHY observations over Park Falls, Wisconsin, J. Geophys. Res., 111, D23302, doi:10.1029/2006JD007080, 2006. 14752

Breon, F. M., Houweling, S., Aben, I., Ehret, G., Chevallier, F., Marshall, J., Flamant, P., Bruneau, D., and Rayner, P.: Observation techniques and mission concepts for the analysis of the carbon cycle, ESA study report Contract No. 20839, ESA, Noordwijk, The Netherlands, 2009. 14744, 14745

Buchwitz, M., Schneising, O., Burrows, J. P., Bovensmann, H., Reuter, M., and Notholt, J.: First direct observation of the atmospheric CO_2 year-to-year increase from space, Atmos. Chem. Phys., 7, 4249–4256, doi:10.5194/acp-7-4249-2007, 2007. 14740

Chahine, M. T., Chen, L., Dimotakis, P., Jiang, X., Li, Q., Olsen, E. T., Pagano, T., Randerson, J., and Yung, Y. L.: Satellite remote sounding of mid-tropospheric CO_2, Geophys. Res. Lett., 35, L17807, doi:10.1029/2008GL035022, 2008. 14740

Chevallier, F.: Impact of correlated observation errors on inverted CO_2 surface fluxes from OCO measurements, Geophys. Res. Lett., 34, L24804, doi:10.1029/2007GL030463, 2007. 14740, 14751

Chevallier, F., Fisher, M., Peylin, P., Serrar, S., Bousquet, P., Breon, F. M., Chedin, A., and Ciais, P.: Inferring CO_2 sources and sinks from satellite observations: method and application to TOVS data, J. Geophys. Res., 110, D24309, doi:10.1029/2005JD006390, 2005. 14742, 14744

Chevallier, F., Viovy, N., Reichstein, M., and Ciais, P.: On the assignment of prior errors in Bayesian inversions of CO_2 surface fluxes, Geophys. Res. Lett., 33, L13802, doi:10.1029/2006GL026496, 2006. 14740

Chevallier, F., Bréon, F.-M., and Rayner, P. J.: Contribution of the Orbiting Carbon Observatory to the estimation of CO_2 sources and sinks: theoretical study in a variational data assimilation framework, J. Geophys. Res., 112, D09307, doi:10.1029/2006JD007375, 2007. 14740

Denning, A. S., Holzer, M., Gurney, K. R. et al.: Three-dimensional transport and concentration of SF_6: A model intercomparison study (Transcom 2), Tellus B, 51, 266–297, 1999. 14741

Deutscher, N. M., Griffith, D. W. T., Bryant, G. W., Wennberg, P. O., Toon, G. C., Washenfelder, R. A., Keppel-Aleks, G., Wunch, D., Yavin, Y., Allen, N. T., Blavier, J.-F., Jiménez, R., Daube, B. C., Bright, A. V., Matross, D. M., Wofsy, S. C., and Park, S.: Total column CO_2 measurements at Darwin, Australia site description and calibration against in situ aircraft profiles, Atmos. Meas. Tech. Discuss., 3, 989–1021, doi:10.5194/amtd-3-989-2010, 2010. 14747,

ACPD
10, 14737–14769, 2010

14759
Ehret, G. and Kiemle, C.: Requirements definition for future DIAL instruments, Study report ESA-CR(P)-4513, ESA, Noordwijk, The Netherlands, 2005. 14740
Engelen, R. J., Denning, A. S., Gurney, K. R., and TransCom3 modelers: On error estimation in atmospheric CO_2 inversions, J. Geophys. Res., 107, 4635, doi:10.1029/2002JD002195, 2002. 14741
Feng, L., Palmer, P. I., Bösch, H., and Dance, S.: Estimating surface CO_2 fluxes from space-borne CO_2 dry air mole fraction observations using an ensemble Kalman Filter, Atmos. Chem. Phys., 9, 2619–2633, doi:10.5194/acp-9-2619-2009, 2009. 14740
GLOBALVIEW-CO2: Cooperative Atmospheric Data Integration Project – Carbon Dioxide, CD-ROM [Also available on Internet via anonymous FTP to ftp.cmdl.noaa.gov, Path: ccg/co2/GLOBALVIEW], NOAA-ESRL, Boulder, Colorado, 2009. 14747
Gurney, K. R., Law, R. M., Denning, A. S., et al.: Towards robust regional estimates of CO_2 sources and sinks using atmospheric transport models, Nature, 415, 626–630, 2002. 14741
Heimann, M. and Körner, S.: The global atmospheric tracer model TM3, Model description and user's manual Release 3.8a, Max Planck Institute of Biogeochemistry, 2003. 14760
Hourdin, F., Musat, I., Bony, S., et al.: The LMDZ4 general circulation model: climate performance and sensitivity to parametrized physics with emphasis on tropical convection, Clim. Dynam., 27, 787–813, 2006. 14760
Houweling, S., Breon, F.-M., Aben, I., Rödenbeck, C., Gloor, M., Heimann, M., and Ciais, P.: Inverse modeling of CO_2 sources and sinks using satellite data: a synthetic inter-comparison of measurement techniques and their performance as a function of space and time, Atmos. Chem. Phys., 4, 523–538, doi:10.5194/acp-4-523-2004, 2004. 14740
Houweling, S., Hartmann, W., Aben, I., Schrijver, H., Skidmore, J., Roelofs, G.-J., and Breon, F.-M.: Evidence of systematic errors in SCIAMACHY-observed CO_2 due to aerosols, Atmos. Chem. Phys., 5, 3003–3013, doi:10.5194/acp-5-3003-2005, 2005. 14751
Ingmann, P.: A-SCOPE, Advanced space carbon and climate observation of planet earth, Report for Assessment, SP-1313/1, ESA communication production office, Noordwijk, The Netherlands, 2009. 14741, 14750
Jiang, X., Li, Q., Liang, M.-C., Shia, R.-L., Chahine, M. T., Olsen, E. T., Chen, L. L., and Yung, Y. L.: Simulation of upper tropospheric CO_2 from chemistry and transport models, Global Biogeochem. Cy., 22, GB4025, doi:10.1029/2007GB003049, 2008. 14752
Kadygrov, N., Maksyutov, S., Eguchi, N., Aoki, T., Nakazawa, T., Yokota, T., and Inoue, G.:

ACPD
10, 14737–14769, 2010

Role of simulated GOSAT total column CO_2 observations in surface CO_2 flux uncertainty reduction, J. Geophys. Res., 114, D21208, doi:10.1029/2008JD011597, 2009. 14740, 14751

Krol, M., Houweling, S., Bregman, B., van den Broek, M., Segers, A., van Velthoven, P., Peters, W., Dentener, F., and Bergamaschi, P.: The two-way nested global chemistry-transport zoom model TM5: algorithm and applications, Atmos. Chem. Phys., 5, 417–432, doi:10.5194/acp-5-417-2005, 2005. 14760

Law, R. M., Peters, W., Rödenbeck, C., et al.: TransCom model simulations of hourly atmospheric CO_2: Experimental overview and diurnal cycle results for 2002, Global Biogeochem. Cy., 22, GB3009, doi:10.1029/2007GB003050, 2008. 14741, 14744

Macatangay, R.: Atmospheric Carbon Dioxide: Retrieval from ground-based fourier from ground-based fourier transform infrared solar absorption measurements and modelling using a coupled global-regional scale approach, Ph.D. thesis, Bremen University, Bremen, Germany, 2010. 14759

Macatangay, R., Warneke, T., Gerbig, C., Körner, S., Ahmadov, R., Heimann, M., and Notholt, J.: A framework for comparing remotely sensed and in-situ CO_2 concentrations, Atmos. Chem. Phys., 8, 2555–2568, doi:10.5194/acp-8-2555-2008, 2008. 14741

Matsueda, H., Inoue, H. Y., and Ishii, M.: Aircraft observations of carbon dioxide at 8-13 km altitude over the Western Pacific from 1993 to 1999, Tellus B, 54, 2–20, 2002. 14752

Meirink, J.-F., Bergamaschi, P., Frankenberg, C., d'Amelio, M. T. S., Dlugokencky, E. J., Gatti, L. V., Houweling, S., Miller, J. B., Röckmann, T., Villani, M. G., and Krol, M. C.: Four-dimensional variational data assimilation for inverse modeling of atmospheric methane emissions: analysis of SCIAMACHY observations, J. Geophys. Res., 113, D17301, doi:10.1029/2007JD009740, 2008a. 14742

Meirink, J. F., Bergamaschi, P., and Krol, M. C.: Four-dimensional variational data assimilation for inverse modelling of atmospheric methane emissions: method and comparison with synthesis inversion, Atmos. Chem. Phys., 8, 6341–6353, doi:10.5194/acp-8-6341-2008, 2008b. 14744

Miller, C. E., Crisp, D., DeCola, P. L., et al.: Precision requirements for space-based xCO_2 data, J. Geophys. Res., 112, D10314, doi:10.1029/2006JD007659, 2007. 14740

Pak, B. C. and Prather, M. J.: CO_2 source inversions using satellite observations of the upper troposhere, Geophys. Res. Lett., 28, 4571–4574, 2001. 14740

Parazoo, N. C., Denning, A. S., Kawa, S. R., Corbin, K. D., Lokupitiya, R. S., and Baker, I. T.: Mechanisms for synoptic variations of atmospheric CO_2 in North America, South Amer-

ACPD
10, 14737–14769, 2010

ica and Europe, Atmos. Chem. Phys., 8, 7239–7254, doi:10.5194/acp-8-7239-2008, 2008. 14747

Patra, P., Law, R. M., and Peters, W.: TransCom model simulations of hourly atmospheric CO_2: analysis of synoptic-scale variations for the period 2002–2003, Global Biogeochem. Cy., 22, GB4013, doi:10.1029/2007GB003081, 2008. 14741

Peters, W., Jacobson, A. R., Sweeney, C., et al.: An atmospheric perspective on North American carbon dioxide exchange: CarbonTracker, P. Natl. Acad. Sci., 104, 18925–18930, 2007. 14742, 14744

Rayner, P. J. and O'Brien, D. M.: The utility of remotely sensed CO_2 concentration data in surface source inversions, Geophys. Res. Lett., 28, 175–178, 2001. 14739, 14740

Rayner, P. J., Law, R. M., O'Brien, D. M., Butler, T. M., and Dilley, A. C.: Global observations of the carbon budget 3. Initial assessment of the impact of satellite orbit, scan geometry, and cloud on measuring CO_2 from space, J. Geophys. Res., 107, 4557, doi:10.1029/2001JD000618, 2002. 14740

Rödenbeck, C., Houweling, S., Gloor, M., and Heimann, M.: CO_2 flux history 1982–2001 inferred from atmospheric data using a global inversion of atmospheric transport, Atmos. Chem. Phys., 3, 1919–1964, doi:10.5194/acp-3-1919-2003, 2003. 14744

Tarantola, A.: Inverse Problem Theory, and Methods for Model Parameter Estimation, Society for Industrial and Applied Mathematics, Philadelphia, 2005. 14742

Washenfelder, R. A., Toon, G. C., Blavier, J.-F., Yang, Z., Allen, N. T., Wennberg, P. O., Vay, S. A., Matross, D. M., and Daube, B. C.: Carbon dioxide column abundances at the Wisconsin Tall Tower site, J. Geophys. Res., 111, D22305, doi:10.1029/2006JD007154, 2006. 14759

Yang, Z., Washenfelder, R. A., Keppel-Aleks, G., Krakauer, N.-Y., Randerson, J. T., Tans, P. P., Sweeney, C., and Wennberg, P. O.: New constraints on Northern Hemisphere growing season net flux, Geophys. Res. Lett., 34, L12807, doi:10.1029/2007GL029742, 2007. 14740, 14741, 14752

Yokota, T., Oguma, H., Morino, I., and Inoue, G.: A nadir looking SWIR FTS to monitor the CO_2 column density for the Japanese GOSAT project, in: Proc. 24th Int. Symp. Space Technol. and Sci., edited by JSASS and of the 24th ISTS, O. C., 887–889, 2004. 14740

ACPD

10, 14737–14769, 2010

Table 1. Overview of FTS sites.

Site	Longitude (deg. east)	Latitude (deg. north)	Data version (GFIT, date)	Institution	Reference
Bremen, Germany	8.85	53.11	2.40.2	iUP-Bremen	Macatangay (2010)
Darwin, Australia	130.57	−12.42	4.4.0 (7 Oct 2009)	Caltech, UoW	Deutscher et al. (2010)
Park Falls, USA	−90.27	45.93	4.4.0 (18 Feb 2009)	Caltech, JPL	Washenfelder et al. (2006)
Spitsbergen, Norway	11.92	78.92	2.40.2	iUP-Bremen	Macatangay (2010)

ACPD
10, 14737–14769, 2010

Table 2. Overview of participating models.

Model	Horizontal resolution	Vertical layers	Meteorology	Optimization	Reference
IFS	125×125 km^2	60η	ECMWF	–	http://www.ecmwf.int/research/ifsdocs/CY31r1/index.html
LMDZv3	3.75°×2.5°	19η	ECMWF (nudged)	variational	Hourdin et al. (2006)
TM3	5°×4°	19σ	NCEP	variational	Heimann and Körner (2003)
TM5	3°×2°	19η	ECMWF	variational	Krol et al. (2005)

ACPD
10, 14737–14769, 2010

Table 3. Boundary and initial conditions specified to all models.

	Prior	Prior uncertainty	Space correlation	Time correlation
Land flux	CarbonTracker	2×CASA r_{het}	250 km	1 month
Ocean flux	CarbonTracker	0.1 g C m^{-2} day^{-1}	1000 km	3 months
Initial conc.	3 yr TM5 spin-up	3.8 ppm on xCO_2	1000 km	–

r_{het}=heterotrophic respiration

ACPD
10, 14737–14769, 2010

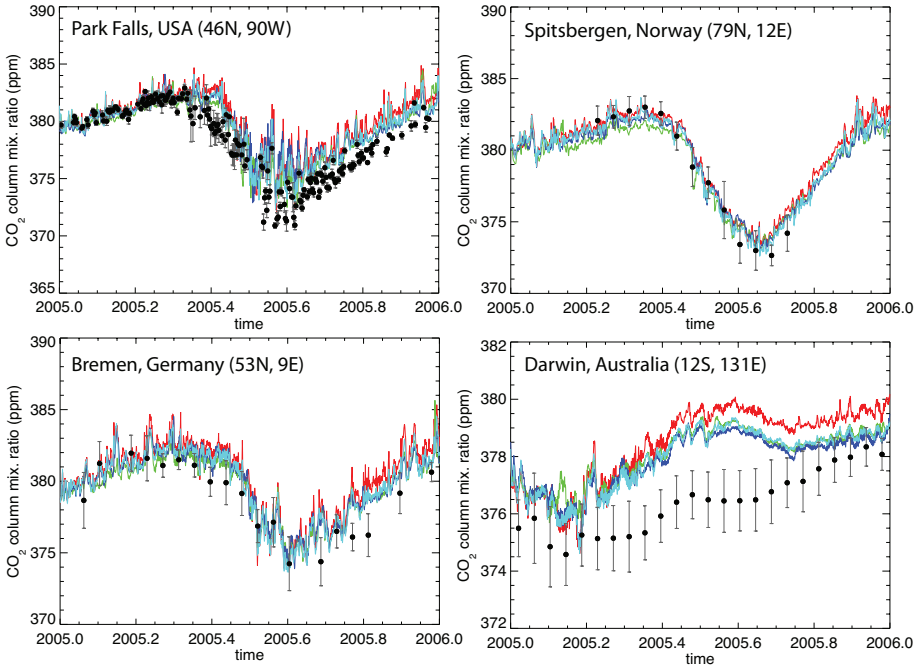

Fig. 1. Comparison between model-simulated and FTS measured xCO_2. Red, IFS; Green, LMDZ; Blue, TM3; Cyan, TM5; Black, measurements. For Park Falls, the measurements represent daily averages, plotted with their 1 σ variability within the day. At the other sites the measurements represent half monthly averages reconstructed from the available years of data (see text). Here the 1 σ intervals represent the variability of the measurements within each half monthly average.

ACPD
10, 14737–14769, 2010

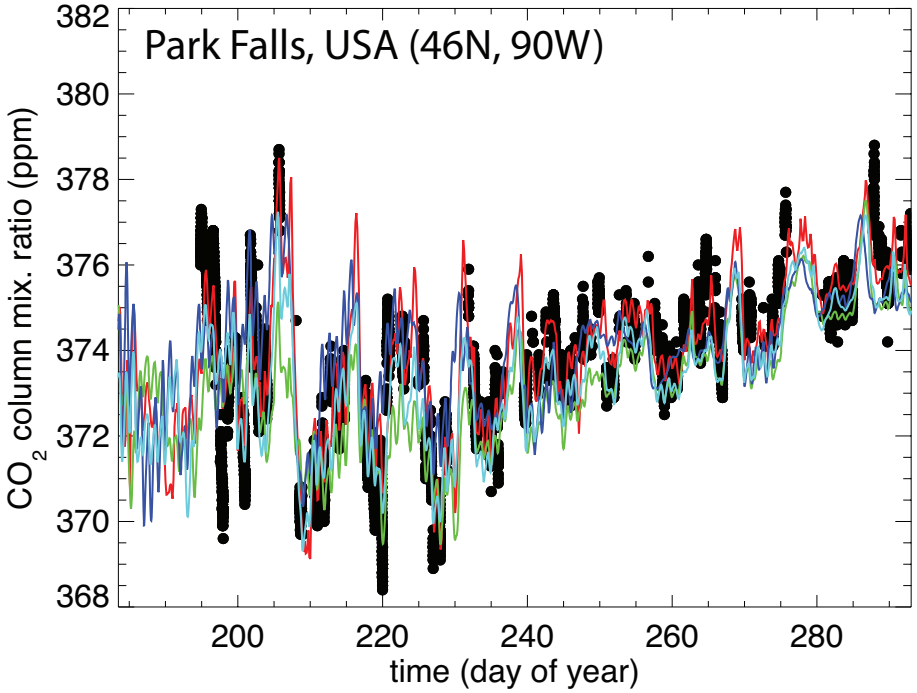

Fig. 2. Same as Fig. 1 zooming in on short-term variability. In this figure the black dots represent FTS measurements without averaging.

ACPD
10, 14737–14769, 2010

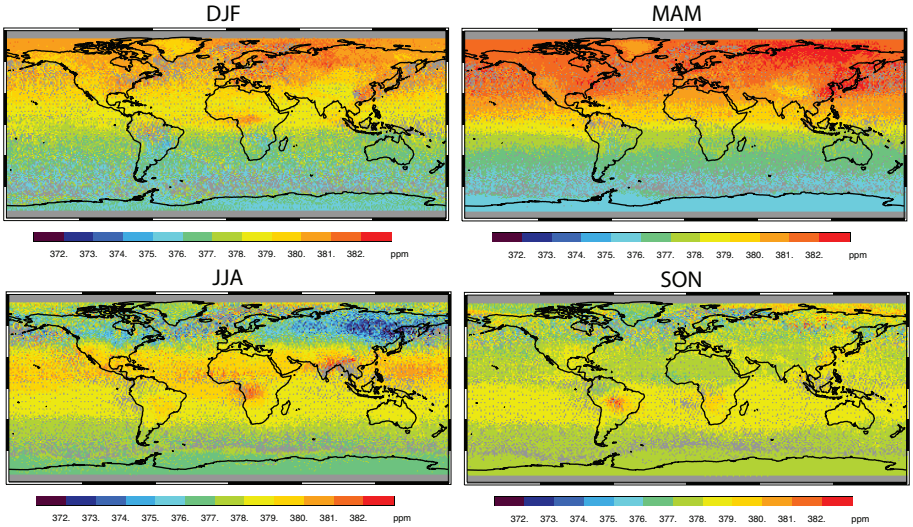

Fig. 3. Seasonal variation in xCO_2 representing the mean of all models sampled like A-SCOPE for the year 2005.

ACPD
10, 14737–14769, 2010

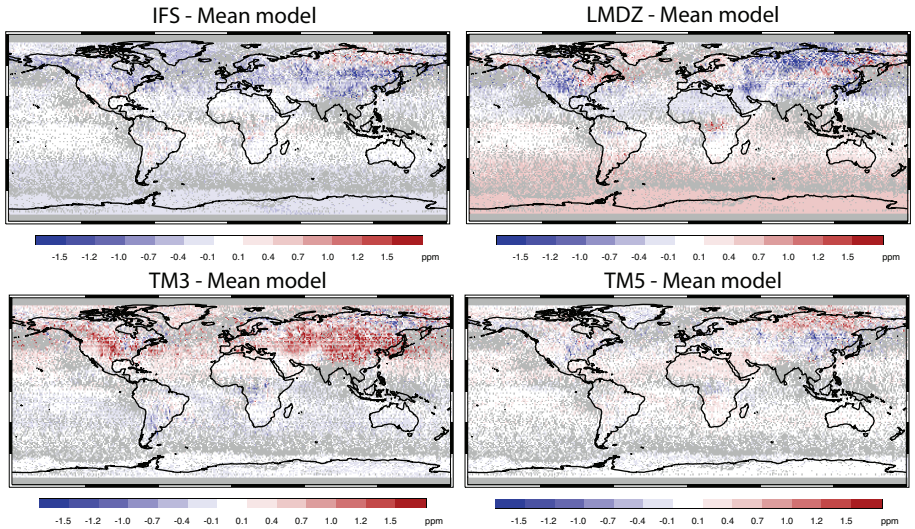

Fig. 4. The difference in xCO_2 between each model and the mean model for July 2005, using A-SCOPE sampling.

ACPD
10, 14737–14769, 2010

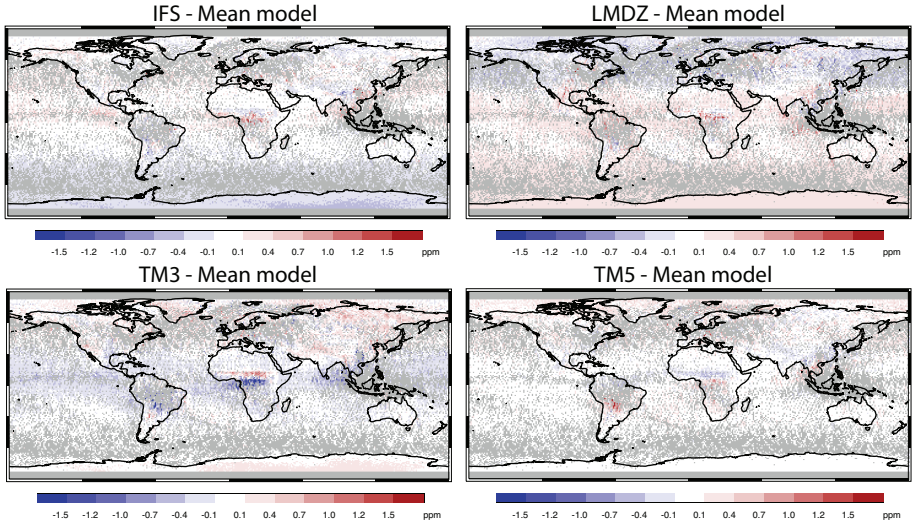

Fig. 5. As Fig. 4 for December 2005.

ACPD
10, 14737–14769, 2010

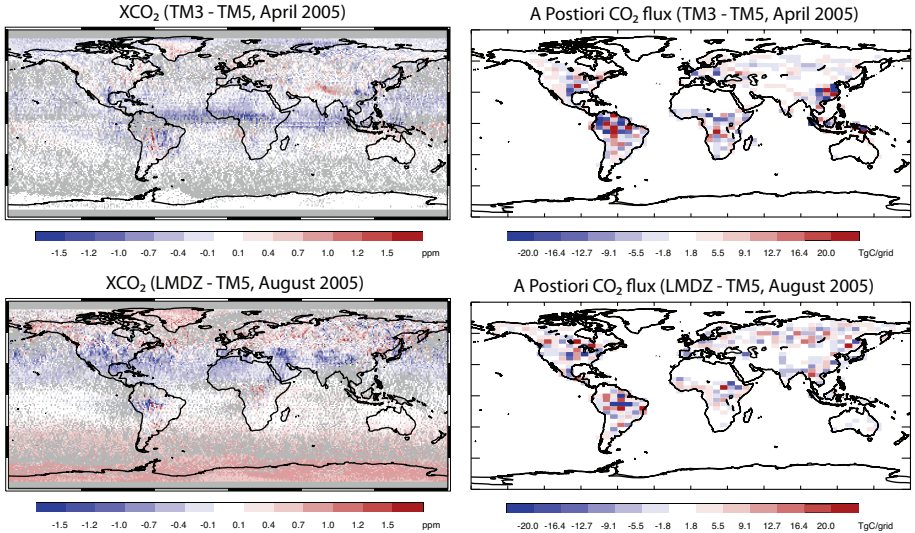

Fig. 6. Examples of the inversion-derived mapping of concentration differences to flux differences. (top panels) TM5 inversion using TM3-derived xCO_2 samples for April, (bottom panel) TM5 inversion using LMDZ-derived xCO_2 samples for August.

ACPD
10, 14737–14769, 2010

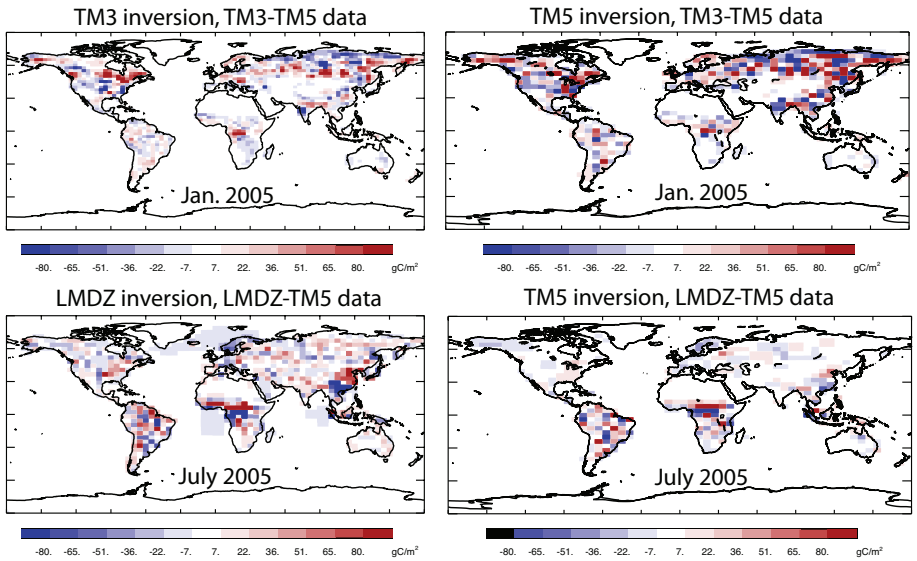

Fig. 7. Examples fluxes derived from different inversion using the same samples. (top panels) TM5 and TM3 inversion using the difference between TM5 and TM3 derived A-SCOPE samples for January, (bottom panels) TM5 and LMDZ inversion using the difference between TM5 and LMDZ derived A-SCOPE samples for July.

ACPD
10, 14737–14769, 2010

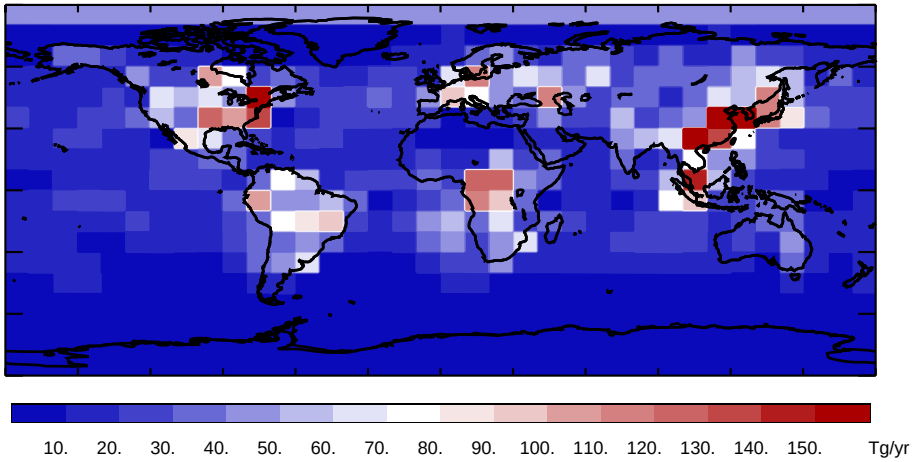

Fig. 8. Flux uncertainties (1σ) for the annual CO_2 flux at 10^6 km^2 as a result of transport model uncertainties.

ACPD
10, 14737–14769, 2010